575. Vibroacoustic frequency response on a passenger compartment

Iulian LUPEA[1], Robert SZATHMARI [2]
[1]Technical University of Cluj-Napoca,
[2]P+Z Engineering
e-mail: *Iulian.Lupea@mep.utcluj.ro*[1]

(Received 30 September 2010; accepted 9 December 2010)

Abstract: The paper presents frequency response analysis at the passenger compartment level followed by an acoustic analysis performed by means of finite element method. Normal mode analysis of the body in white (BIW) was performed and the eigenvectors presented. A frequency-dependent velocity excitation profile in vertical direction at the front and rear axles were considered for the frequency response analysis. The acceleration response at three driver comfort points was recorded as well. Subsequently, in the coupled fluid-structure frequency response analysis the calculation of sound pressure level (SPL) variation as a function of the same frequency-dependent load was conducted at the driver and rear passenger ear locations. The paper is finalized with conclusions on the comfort driver points and sound pressure levels as response to the in-phase and out-of-phase frequency dependent excitation. This analysis is a prerequisite for structural panel participation and structure optimization.

Keywords: modal analysis, modal frequency response, acoustic analysis, body in white, passenger compartment.

1. INTRODUCTION

The reduction of interior vibration and noise in automobile passenger compartments is of continuous interest. Vibrations and noise are generated from tires, wind, engine, transmission as well as from the exhaust system, and transmitted through the body structure to the comfort points and to the air of the passenger compartment.
CAE tools are playing a paramount role in the process of vehicle structure development. Starting from the 3D geometry, the car structure is meshed by using proper finite elements. In the development of the body in white (BIW) structure, the frequency response analysis is an important building block in ensuring the functional characteristics. Car structure dynamic model based on resonance frequencies, damping ratios and mode shapes is the target of the structural modal analysis [1,5].

In the car model under study, the compartment is filled with air, which is coupled with the BIW structure. The trimmed body and seats are neglected because the movement of main structural panels is targeted. Also, we are looking for acoustic results due to the movement of these panels. Thereby we can optimize the topology, topography or thickness of the parts. Structural modifications can change vibration load paths as well. For additional components (seats, interior and exterior accessories) we can take in consideration their participation in the mass and stiffness matrix. Hence, in the finite element model one can use concentrated masses or non-structural masses, which can be connected with constraints to the model, simulating the real connection of these parts, thus reducing the computation time.

The sound field of the compartment is influenced by acoustic modal features of the enclosed cabin, dynamic characteristic of the surrounding structure that transfer the excitation from the main sources [2, 3, 7].

In the simulation, the passenger compartment air-structure interaction is considered. The air is coupled with the (wetted) structure which touches the boundary fluid elements.

2. NORMAL MODE ANALYSIS OF THE CAR STRUCTURE

2.1 The eigenvalue problem

Dynamical equations of mechanical systems can be written in matrix form as follows:

$$M\ddot{Q} + C\dot{Q} + KQ = F \tag{1}$$

where Q is the vector of the m system generalized coordinates or the finite element degrees of freedom, $M, C, K \in \Re^{mxm}$ are the mass (inertia), damping and stiffness matrices and F is the vector of generalized forces. The matrices M, C and K are considered symmetrical.

Assuming a synchronous motion in the structure nodes, the following solution is proposed:

$$Q(t) = u\, e^{i\omega t} \tag{2}$$

where ω is a natural frequency of the whole system harmonic vibration, $i = \sqrt{-1}$ and u is a constant n–vector of amplitudes. Substituting in (1) the proposed solution and neglecting damping and the external forces, results in:

$$Ku - \omega^2 Mu = 0 \;\; or \;\; (K - \omega^2 M) \cdot u = 0 \tag{3}$$

The set of obtained homogeneous algebraic equations (3) has the unknown vector u. Considering $\lambda = \omega^2$ as a parameter we get:

$$Ku = \lambda Mu \tag{4}$$

known as the eigenvalue problem when trying to determine λ values. By solving for λ and nontrivial ($u \neq 0$) solution, the following characteristic equation (5) after premultiplying with M^{-1}, is obtained:

$$\det(M^{-1}K - \lambda I) = 0 \tag{5}$$

where λ_r $(r=1,..,n)$ values are the eigenvalues or characteristic values of the system and M is positive definite. For each determined eigenvalue λ_r an associated eigenvector u_r (defining a mode shape) is satisfying the following equation:

$$Ku_r = \lambda_r Mu_r \quad r = 1,2,...,n \tag{6}$$

2.2 Normal mode analysis

The modal analysis of the car structure has been performed by using Nastran. The damping being neglected, the natural or undamped natural modes of vibration have been derived.

The natural modes of vibration in 0-50 Hz interval, are shown in Table 1. This interval is chosen due to the presence of the revealing modes in this range for most passenger auto vehicles. By revealing modes we mean Bending 1, Bending 2, side Bending, Torsion 1 and Torsion 2 modes (Fig. 1-3) (specific for a bar-shaped structure), which can be used further for optimization. Knowing the major modes, after frequency response analysis, for optimization we can observe only the shift in frequency of these modes (by running a simple modal analysis). Thus, the computation and work time is reduced. Later, for acoustic analysis, during the optimization process, one can observe the local movements of some parts (their influence on the sound pressure) hence, we can stiffen only the parts of interest without shifting significantly the natural frequencies of the major modes [6].

Table 1. List of the modes of vibration under 50Hz

Mode #	Freq [Hz]	Description
1	26,9	Movement of front end, rear end and floor panels in Z direction (pumping).
2	27,4	Torsion 1 (Fig. 1)
3	31,0	Side bending of front end, pumping of floor panel and roof panel and movement in Z direction of rear end.
4	32,0	Bending 2 (Fig. 2)
5	36,4	Bending 1 (Fig. 3)
6	37,8	Movement of front end in Y direction, rear end, and floor panels in Z direction (pumping); movements of A and B beams in Y direction, deformation of trunk compartment.
7	39,3	Movement of front end in Z direction, rear end in Z direction, and floor panels in Z direction (pumping); movements of A, B and C beams, deformation of the trunk compartment.
8	43,7	Movement of front end in Y and Z directions, rear end in Z direction, and floor panels in Z direction (pumping); movements of A, B and C beams, deformation of trunk compartment, movement of windows.
9	44,8	Movement of front end in Y and Z directions, rear end in Z direction, and floor panels in Z direction (pumping), torsion of main structure.
10	49,9	Movement of front end in Y and Z directions, rear end in X direction, torsion of main structure, pumping of front and rear windows, strong deformation of rear compartment.

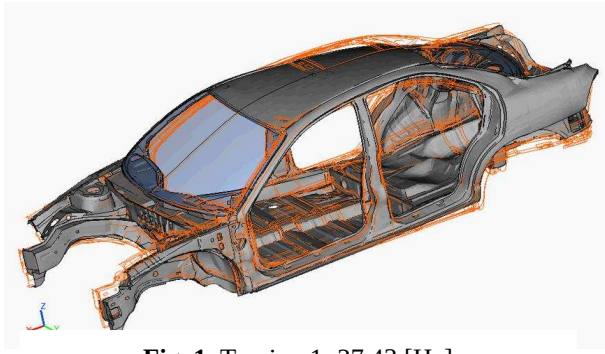

Fig. 1. Torsion 1: 27,43 [Hz]

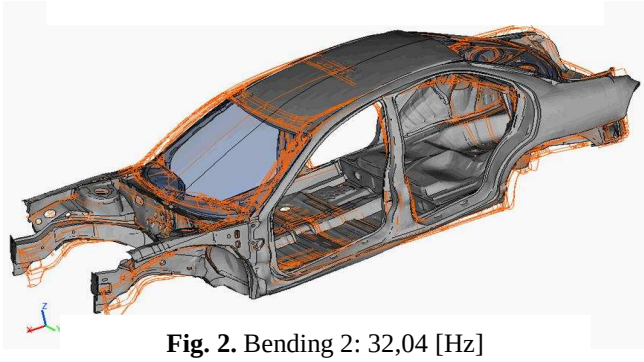

Fig. 2. Bending 2: 32,04 [Hz]

Fig. 3. Bending 1: 36,48 [Hz]

3. FREQUENCY RESPONSE ANALYSIS

3.1. Excitation and responses

For the frequency response analysis we have chosen a velocity excitation, in the frequency bend of 0-80 Hz, which simulates the normal road excitation. From 0 to 5 Hz we have a velocity ramp, followed by a constant velocity excitation of 25 mm/s over the frequency band.

Excitation locations (Fig. 4) are the grids which assimilate the center of the wells and are transmitted to the connection points of the suspension system.

We take in consideration two load cases. In the first case the structure is excited in phase at the two axles, front and rear, and in the second case the two axles are excited out of phase.

The points of interest for the response are three driver comfort points: the right foot of the driver according to the position of the gas pedal, the right connection point of the driver chair with the floorboard (Fig. 5) and the connection point of the rear view mirror with the windscreen (Fig. 6).

For the mentioned comfort points we are looking for the amplitudes of the accelerations, which can be relevant for the recognition of the eigenmodes of the structure in an inverse process of determination of these modes.

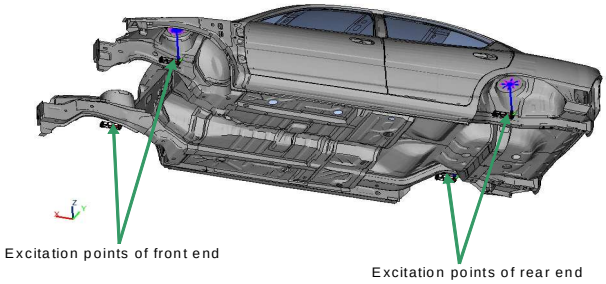

Fig. 4. Excitation points

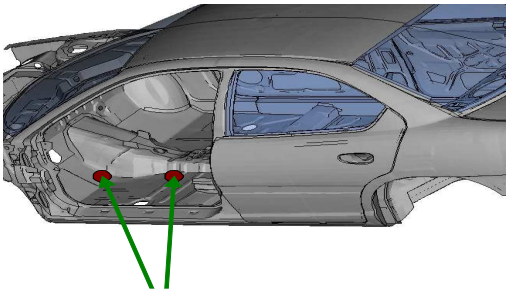

Fig. 5. Comfort points #1, #2

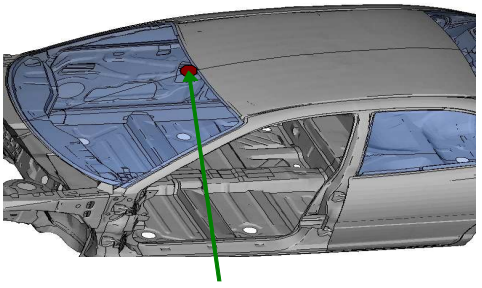

Fig. 6. Comfort point #3

3.2 Direct and Modal Frequency Response Analysis

The direct frequency response method is rarely used, due to the excessive computational time. In the direct method, structural response is computed at discrete excitation frequencies by solving a set of coupled matrix equations. The system of damped and forced vibration equations of motion with harmonic excitation is:

$$M\ddot{Q} + C\dot{Q} + KQ = R(\omega)\, e^{i\omega t} \tag{7}$$

For harmonic excitation, a harmonic response or a complex solution of the form (8) is assumed:

$$Q = u(\omega)\, e^{i\omega t} \tag{8}$$

where $u(\omega)$ is a complex displacement vector to be determined. Taking the first and the second derivatives of (8), substituting them into (7) and dividing by nonzero quantity $e^{i\omega t}$, gives:

$$\left[K - \omega^2 M + i\omega C\right] u(\omega) = R(\omega) \tag{9}$$

which is the matrix form of equations of motion, ω being one of the excitation frequency in the frequency band of interest.

The modal frequency response analysis uses the significant mode shapes of the structure to reduce the system size, to uncouple the equations of motion (when modal or no damping is assumed), and to make the numerical solution more efficient.

The equations of motion (7) were transformed from *m* physical coordinates Q(t) to a subset of *n* modal coordinates $Q_p(t)$ by using the relation:

$$Q = \phi_t\, Q_p \tag{10}$$

where ϕ_t (m x n) is the truncated modal matrix assembling the significant *n* modal vectors ϕ_i:

$$\phi_t = [\phi_1, \phi_2, \ldots, \phi_i, \ldots, \phi_n] \tag{11}$$

and ϕ_i is the i-th modal vector:

$$\phi_i = [\phi_{1i}, \phi_{2i}, \ldots, \phi_{ji}, \ldots, \phi_{mi}]^T$$

The following complex solution is assumed:

$$Q = \phi_t\, \xi(\omega) e^{i\omega t} \tag{12}$$

where $\xi = [\xi_1, \xi_2, \ldots, \xi_k, \ldots, \xi_n]^T$ and $\xi_{k\,(k=1,\ldots,n)}$ is the amplitude of the *k-th* modal coordinate.

The mode shapes are used to transform the problem in terms of the behavior of the modes as opposed to the grid points. By substituting the proposed solution (12) in equation (7), the equation for harmonic motion is as follows:

$$\left[-\omega^2 M\phi_t + i\omega\, C\phi_t + K\phi_t\right]\xi(\omega) = R(\omega) \tag{13}$$

Relation (13) is the equation of motion in matrix form, in terms of the modal coordinates. To uncouple the equations, one can premultiply (13) by ϕ_t^T (n x m) resulting in:

$$\left[-\omega^2 \phi_t^T M\phi_t + i\omega\, \phi_t^T C\phi_t + \phi_t^T K\phi_t\right]\xi(\omega) = \phi_t^T R(\omega) \tag{14}$$

By using the orthogonality property of the mode shapes, the equations of motion in terms of the generalized mass, damping and stiffness matrices (*Mp, Cp, Kp*) are obtained:

$$\begin{aligned} \phi_t^T M \phi_t = M_p \quad \phi_t^T C \phi_t = C_p \\ \phi_t^T K \phi_t = K_p \quad \phi_t^T R(\omega) = R_p \end{aligned} \tag{15}$$

These diagonal matrices do not have the off-diagonal terms that couple the equations of motion, hence the *n* modal equations of motion in matrix format, are uncoupled:

$$\left[-\omega^2 M_p + i\omega C_p + K_p\right]\xi(\omega) = R_p \tag{16}$$

The equations of motion appear to be a set of uncoupled single degree of freedom system. The individual modal response of each eigenmode is computed:

$$\xi_i(\omega) = \frac{1}{-\omega^2 m_{pi} + i\omega c_{pi} + k_{pi}} \cdot r_{pi}(\omega) \tag{17}$$

where m_{pi}, $c_{pi,}$ $k_{pi,}$ $r_{pi}(\omega)$ are the i-th modal mass, modal damping, modal stiffness and modal force respectively. After the modal frequency response analysis with Nastran [9], the accelerations at the driver's comfort locations have been determined. The results for the out-of-phase excitation and for the in-phase excitation are depicted in Fig. 7 and Fig. 8 respectively.

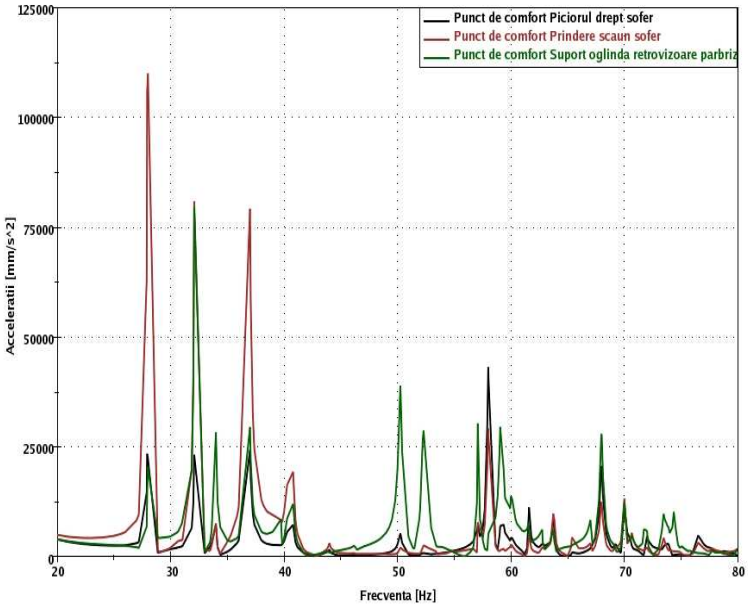

Fig. 7. Response (acc. vs. freq.) - in phase excitation

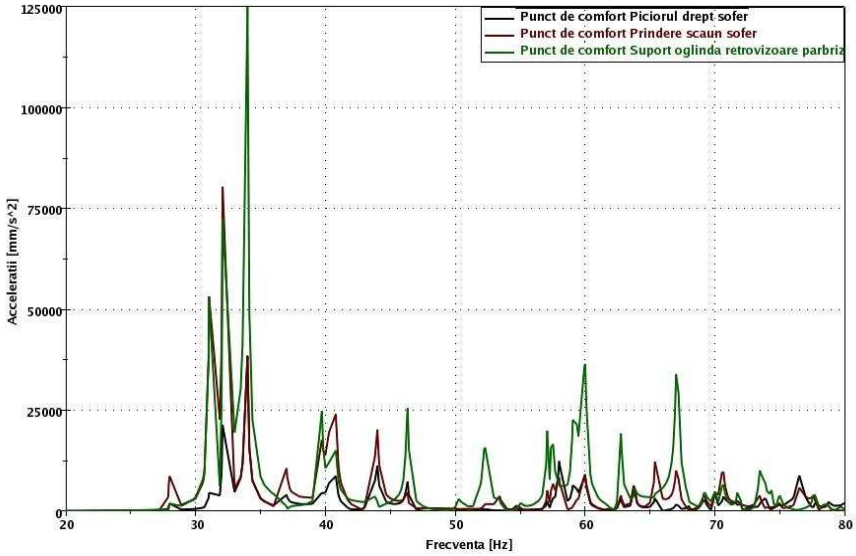

Fig. 8. Response - out of phase excitation

4. ACOUSTIC ANALYSIS

4.1 Normal modes

The acoustic analysis has been performed with MSC Nastran 7. Fluid boundaries may be fixed, flexible or free. With no applied loads, the outer surfaces of the fluid finite elements define a fixed, rigid boundary condition, approximating a normal pressure gradient of zero. If structural finite elements are attached, they will generate flow into the fluid and affect the pressures. The pressure degrees-of-freedom may be treated like displacement degrees-of-freedom. Also, they may be constrained with SPC or MPC for various other reasons, such as symmetry. The parameters of the fluid-structure interfaces have been defined by using the card ACMODL.

The mesh density of the acoustic model should be able to predict modes up to the upper bound of the frequency of interest. The wavelength of an acoustic mode is much longer then a similar one belonging to the structural model in the same frequency band. Hence, the mesh of the acoustic model is coarser than the mesh of the structural model. For the fluid model an average element size of 33 mm has been proposed. We used MAT10 material card to simulate the air in the passenger compartment with the following parameters: bulk modulus, mass density, speed of sound, fluid element damping coefficient and the normalized admittance coefficient for porous material.

If no structure is connected and the problem involves only fluid, then the effects of the boundary flexibility may be ignored and the problem is simplified.

The natural frequencies were obtained from SOL 103 using symmetric real methods at greatly reduced costs.

For a normal mode acoustic analysis and the uncoupled fluid, one can observe the results in the Figs. 9-14. These figures are showing the first and the second longitudinal eigenmodes, the first transversal eigenmode, followed by a combined mode, the third longitudinal eigenmode and in the last figure the first vertical eigenmode. The dark areas are indicating nodes in the pressure ratios.

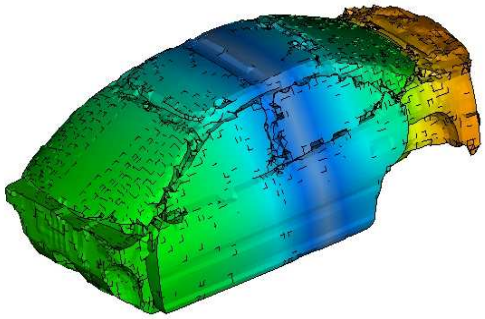

Fig. 9. 1st longitudinal eigenmode (62.2Hz)

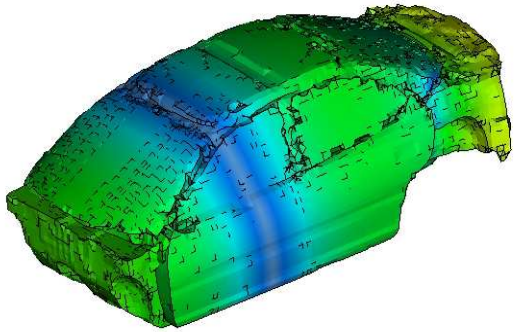

Fig. 10. 2nd longitudinal eigenmode (103 Hz)

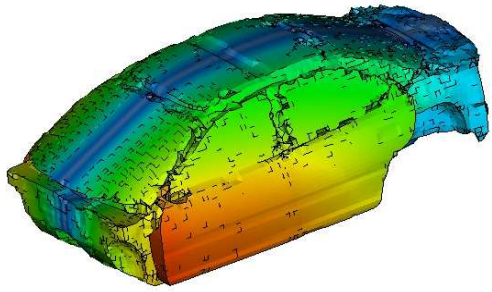

Fig. 11. 1st transversal eigenmode (112 Hz)

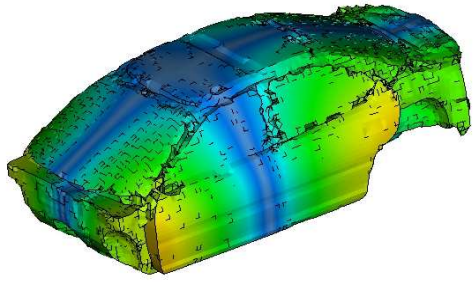

Fig. 12. Combined eigenmode (141 Hz)

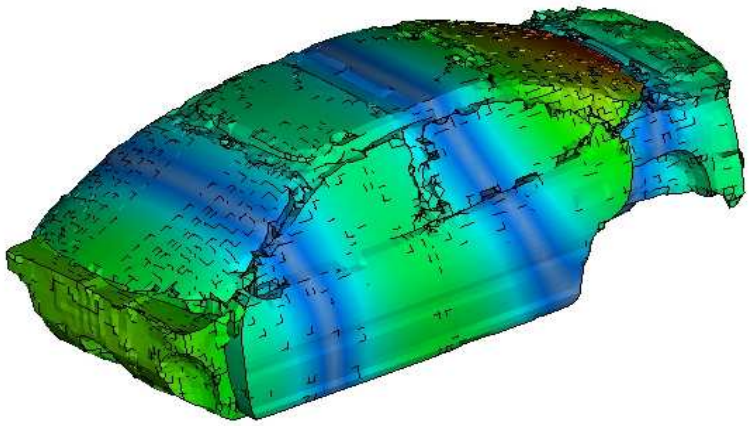

Fig. 13. 3rd longitudinal eigenmode (155 Hz)

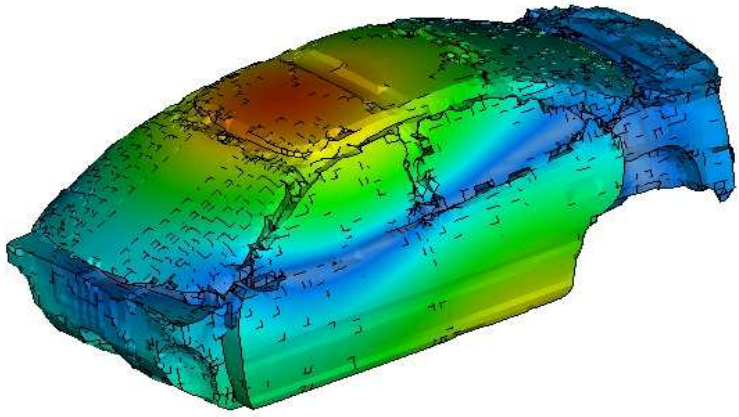

Fig. 14. 1st vertical eigenmode (169Hz)

4.2. COUPLED FLUID-STRUCTURE FREQUENCY RESPONSE ANALYSIS

The target of the acoustic analysis is the calculation of the sound pressure level P_{dBA} variation as a function of a frequency-dependent load:

$P_{dBA} = 20\log(\frac{P/\sqrt{2}}{20\mu Pa}) + A_{weighting}$ where P is predicted by simulation [2, 4].

For the frequency response analysis we have chosen a velocity excitation. This excitation is acting at the front and rear axles having the same profile as in the structural analysis. The system contains the structure and the passenger compartment, both coupled through boundary conditions. At the fluid-structure interface the fluid particles and the structure nodes are moving together following the normal vector to the structure-fluid boundary. The continuity of pressure is also applied. The differential equations of motion of the undamped system dynamics and the coupling between the structure and the acoustic cavity, can be written according to [3] in a matrix form (18):

$$\begin{bmatrix} M_s & 0 \\ \rho c^2 A_{sf}^T & M_p \end{bmatrix}\begin{bmatrix} \ddot{Q}_s \\ \ddot{Q}_p \end{bmatrix} + \begin{bmatrix} C_s & 0 \\ 0 & C_p \end{bmatrix}\begin{bmatrix} \dot{Q}_s \\ \dot{Q}_p \end{bmatrix} + \begin{bmatrix} K_s & -A_{sf} \\ 0 & K_p \end{bmatrix}\begin{bmatrix} Qs \\ Qp \end{bmatrix} = \begin{bmatrix} f_s \\ f_p \end{bmatrix} \quad (18)$$

where Q_s, Q_p and f_p are the structural nodal displacements, acoustic nodal pressures and external force excitation vector respectively. *Ms*, *Cs* and *Ks* are the structural mass, damping and stiffness matrices. *Mp*, *Cp*, *Kp* are the acoustic cavity mass, damping and rigidity matrices. The vector of forces acting on the structure from the fluid region is $f_f = A_{sf} Q_p$, where the matrix A_{sf} describes the spatial coupling between the structure and the acoustic domain. The forces acting on the fluid from the structure are: $f_s = \rho c^2 A_{sf}^T \ddot{Q}_s$, where ρ and c are density and sound speed respectively. For the frequency response analysis of the structure-acoustic system, the following solution is proposed and substituted in (18).

$$\begin{bmatrix} Q_s \\ Q_p \end{bmatrix} = \begin{bmatrix} u_s(\omega) \\ u_p(\omega) \end{bmatrix} e^{i\omega t} \quad (19)$$

where u_s and u_p are the displacement and pressure amplitudes.

The sound pressure level (SPL) is evaluated inside the compartment at two different microphone locations: at the driver ear and at the rear passenger ear (Fig. 15). The target of the analysis is, in general, to evaluate and to reduce the pressure level at the ear locations in the passenger compartment.

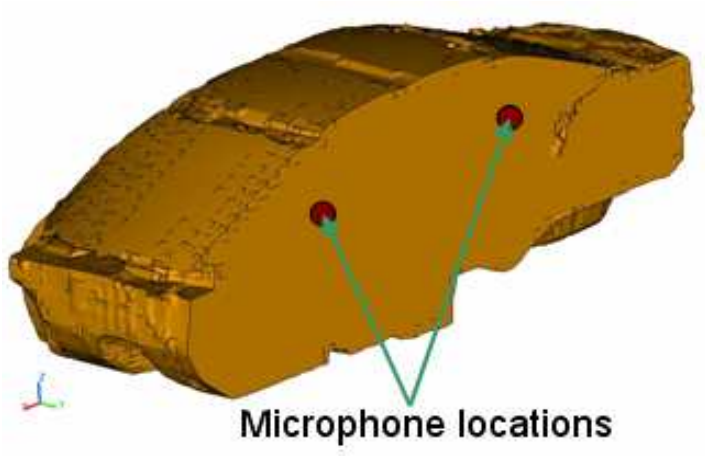

Fig. 15. SPL measuring locations

After running Nastran, the resulting sound pressure levels for the in-phase excitation and for the out-of-phase excitation (at the axles level) are depicted in Fig. 16 and in Fig. 17 respectively.

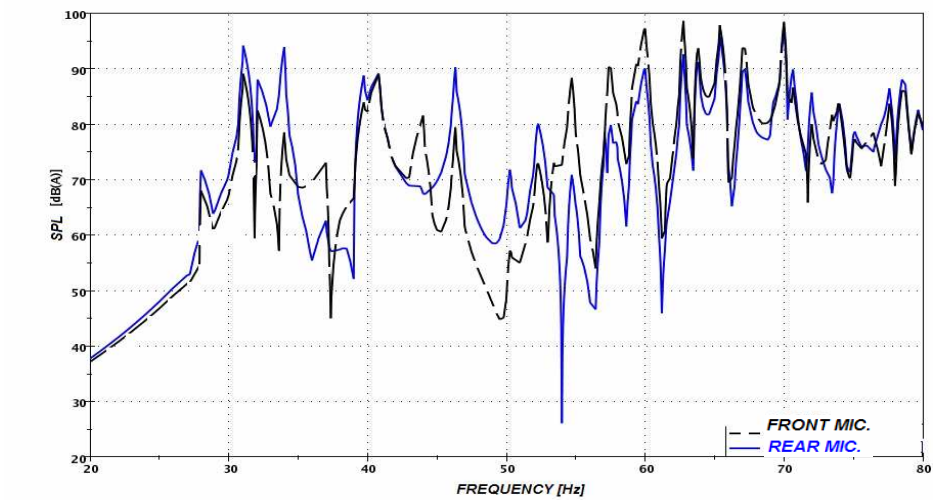

Fig. 16. SPL vs. frequency – in-phase excitation

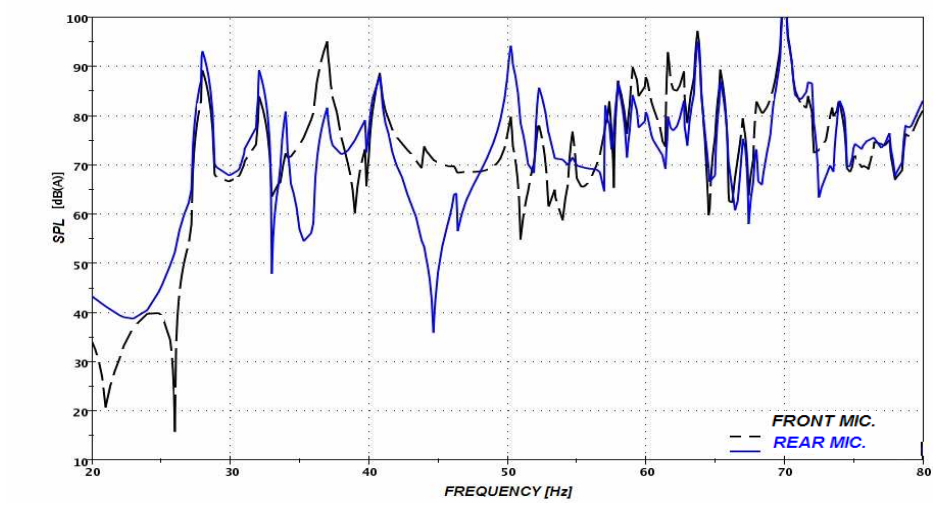

Fig. 17. SPL vs. frequency – out-of-phase excitation

4. CONCLUSIONS

Fig. 7 and Fig. 8 indicate that the maximum response is near the resonant frequencies. For example we can find the maximum amplitude of response for the seat support point near the *bending 1* and *bending 2* also in the range of the *torsion 1 natural frequencies*. Also the magnitude of response is larger in the case of in- phase excitation in comparison to the out-of-phase excitation case. This phenomenon is due to the movement vectors of the floorboard, which is amplified in these modes, as well as due to the fact that in the out-of-phase excitation the load is applied in opposition with the shape of the deformed structure in these eigenmodes. For the mirror point we have the same case regarding the frequency range due to the shape the windscreen is moving in eigenfrequencies and also the difference between the two subcases.

For the right foot point, in both subcases we have lower response due to the position of the point on the tunnel, giving it a high stiffness.

These results can later be used for optimization of the structure by stiffening or flexing the desired part according to the movement in the modes.

Considering the simulation parameters and the model components the SPL calculated is due to the movement of the structural panels only, from which the BIW structure is composed of. In a simulation including the trimmed body the result may differ. Due to the existing masses and additional components which stiffen or loosen the structure, the fluid structure interface will be modified also, due to the higher number of elements which are wetted by the fluid. In this situation more energy is transmitted to the fluid. This energy does not necessarily increase the sound pressure. Depending on the movement of the parts the energy can be transmitted in opposition with other elements, which can result in a decrease of pressure. This analysis is a prerequisite for panel participation and structure optimization.

Phenomena like acoustic absorption and transmission loss encountered in the real structure and trim can be included in the simulation by using acoustic absorber and acoustic barrier finite elements. The resistance, reactance, frequency–dependent impedance and the confidence level of the acoustic materials can be considered, as well in a future work.

5. REFERENCES

[1] Auweraer H. *Structural Dynamics using Modal Analysis: Applications, Trends, and Challenges*, IEEE Instrumentation and Measurement Technology Conference, Budapest, May 21-23, 2001.

[2] Campbell B., Abrishaman M., Stokes W. *Structural-Acoustic Analysis for the Prediction of Vehicle Body Acoustic Sensitivities*, SAE paper 931327, 1993.

[3] Davidsson P., Sandberg G. *A reduction method for structure-acoustic and poroelastic-acoustic problems using interface-dependent Lanczos vectors*, Computer methods in applied mechanics and engineering, 2004.

[4] Kruntcheva M. *Acoustic-structural coupling of the automobile passenger compartment*, Proc. of the World Congress on Engineering 2007 WCE, London, UK, July 2007.

[5] Lupea I. *Vibration and noise measurement by using Labview programming*, Casa Cărții de Știință Publisher, Cluj-Napoca, 2005.

[6] Thomas H., Mandal D., Pagaldipti N. *Optimization to reduce automobile cabin Noise*, EngOpt 2008, Int. Conference on Engineering Optimization, Rio de Janeiro, Brazil, June, 2008.

[7] Virtič M. P., Aberšek B., Župerl U. *Using of Acoustic Models in Mechanical Diagnostics* Strojniški vestnik - Journal of Mechanical Engineering 54(2008)12, 874-882

[8] ** HyperWorks, Altair Eng., Troy, MI..

[9] ** MSC Nastran, User's Manual and Quick Reference Guide; MSC Software Corporation.